

Plasmon resonance of gold nanorods for all-optical drawing of liquid droplets

M. de Angelis,^{1,a)} P. Matteini,¹ F. Ratto,¹ R. Pini,¹ S. Coppola,² S. Grilli,² V. Vespi, ² and P. Ferraro²

¹CNR - Istituto di Fisica Applicata "Nello Carrara," via Madonna del Piano 10, 50019 Sesto Fiorentino (FI) Italy

²CNR - Istituto Nazionale di Ottica sez. di Napoli, via Campi Flegrei 34 Comprensorio "A. Olivetti," 80078 Pozzuoli (NA) Italy

(Received 30 July 2013; accepted 30 September 2013; published online 17 October 2013)

We present a laser-assisted system for dispensing liquid micro-droplets by near infrared illumination of a pyroelectric crystal functionalized with gold nanorods embedded into polyvinyl alcohol. The non-invasive near infrared source resonates with the plasmon oscillations of the gold nanorods, providing a controlled thermal stimulus able to generate the pyroelectric effect. The resulting electric field interacts electro-hydrodynamically with a liquid reservoir leading to precise drawing of micro-litre droplets. This laser-assisted electro-hydrodynamic technique may open the way to the development of more compact and non-invasive nano-dispensing devices. © 2013 AIP Publishing LLC. [<http://dx.doi.org/10.1063/1.4825337>]

Lab-on-a-chip systems are of great interest in biotechnological and chemical applications, thanks to their possibility of producing the desired products faster and in greater yield and purity compared to conventional techniques.¹ Basically two main classes of microfluidic approaches have been developed during the last decades. The continuous flow microsystems² usually consist of a network of micrometre-sized channels, thus suffering from various drawbacks, including large dead volumes and obstruction of channels. Moreover, they make use of valves and pumps, which increases complexity, cost and fragility of the system. On the other hand, the so-called "digital microfluidics" (Ref. 3) confine the reactions into single droplets, even with high monodispersivity.⁴ A significant advantage of droplet-based systems is that they are compatible with wall-free structures, so that the operations can conveniently be performed on the surface of a planar substrate. Surface microfluidics are simpler to fabricate and assemble and, lacking fixed microchannels, they can be reconfigured more easily. A number of techniques have been proposed for the actuation of microfluidic droplets, including the use of thermocapillary effects,⁵ electrochemical gradients,⁶ photochemical effects,⁷ and dielectrophoresis.⁸ More recently, the same authors developed an innovative platform for actuating microdroplets through pyroelectric activation of the dielectrophoresis, with additional advantages in terms of versatility.^{9,10} In this framework, precise and reliable droplet dispensers are highly desirable and different techniques have been presented in literature. Some of these rely on fluid interface instabilities,¹¹ or on atomic force probes.¹² Other approaches involve electrohydrodynamic jetting through appropriate nozzles.¹³ These electric field based methods provide droplets with relatively high resolution but require the arrangement of appropriate electrodes and high voltage circuits and the fabrication of micrometric nozzles. Recently, the same authors have developed a pyro-electrohydrodynamic (P-EHD) approach for different applications, including liquid printing in the

attolitre volume range,¹⁴ fabrication of solid photonic microstructures,¹⁵ manipulation of dielectric micro-targets.¹⁶ In those works, the electric field, responsible for the electrode-free and nozzle-free manipulation of liquids, polymers, and solids, was activated onto lithium niobate (LN) and lithium tantalate (LT) crystals by resistive sources (e.g., hot tip of a soldering iron) that were contact-dependent, or by CO₂ lasers that avoided contact thanks to the absorption of those crystals in the far infrared (IR) region but sacrificing the compactness and making difficult the beam alignment due to invisibility to the naked eye.

Here, we propose a laser-assisted EHD (LA-EHD) technique based on the successful combination of a near infrared (NIR) source with the plasmon resonance of gold nanorods (GNRs) patterned onto the surface of a LN crystal. This system exhibits additional advantages compared to the electrode- and nozzle-free pyro-EHD configuration developed previously by the same authors.¹⁴ The stimulation of the pyro-EHD effect is performed optically by a compact laser source launched in fibre. Such fibre-based setup favours the integrability and makes the light addressing easier thanks to its visibility to the naked eye when the light hits the target. In this context, a portable system could be fabricated for bio-sensing applications where on site drawing of very little amounts of liquids is needed. More versatile dispensing modes (serial and multiple) are possible by simply modulating the distance between fibre and crystal and therefore by lens-free manipulation of the beam expansion. Moreover, additional versatility and precision are provided here by the possibility of patterning the heat source onto the pyroelectric crystal. In fact, the thermal gradient is ensured by the efficient photothermal conversion of the GNRs during the plasmon resonance induced by laser illumination, so that the pyroelectric effect can be generated with high precision and selectivity by near field excitation through an appropriately addressed small beam or alternatively by a largely expanded beam illuminating a pattern of GNRs. The selectivity offered by the patterning approach reduces the stress induced to the crystal and provides, at the same time, better control over the

^{a)}Electronic mail: m.deangelis@ifac.cnr.it

excitation process. In addition, the use of NIR light minimizes undesirable absorption from solvents and reagents, which occurs usually in case of visible and IR frequencies, thus producing undesirable signals. Moreover, compared to the far IR output of a CO₂ laser, with a 20-fold smaller wavelength, NIR light may be focused to smaller spots on the crystal, thus improving the spatial resolution and therefore the control of the dispensing process. The thermal gradient can be induced with relatively high accuracy by modulating the laser power with high spatial selectivity.¹⁷

Such GNRs have been extensively used in a broad range of applications because of their unique optical and photothermal properties.¹⁸ Their optical response originates from sharp plasmonic resonances which give rise to two intense bands centered in the green and NIR windows. The GNRs are much more stable under luminous excitation than conventional dyes.¹⁸ This property has been recently exploited for engineering multifunctional nanocomposites where the photothermal conversion triggers additional functions such as adhesion and chemical release.^{17,19,20} Here, a diode laser emitting at 810 nm was used for exciting the GNRs that therefore provide efficient photothermal conversion and sustain a local heating.

GNR is synthesized by seed-mediated autocatalytic reduction of chloroauric acid with ascorbic acid in the presence of cetrimonium bromide and silver nitrate, according to a variant of the method by Nikoobakht and El-Sayed.^{21,22} Thereafter particles are dispersed at the rate of 20 mM Au into a viscous aqueous solution containing 50 μ M cetrimonium bromide and 6% (w/w) polyvinyl alcohol (PVA).²³

Droplets of this suspension with volumes of about 2 μ l are casted onto LN wafers (z-cut, optically polished and 500 μ m thick from Crystal Technology, Inc.) after cleansing with acetone and ethanol in an ultrasound bath and left to dry at room temperature overnight under a hood. The final films of GNR and PVA contain 400 mM Au on average, which originates from a loss of volume by 95% upon dehydration of the original aqueous suspension. Their thickness ranges between 20 and 50 μ m (see Fig. 2). However, we acknowledge that these concentrations and thicknesses proved inhomogeneous because of the so-called coffee stain effect.²⁴

The preservation of GNR optical response has been checked in order to ensure reproducible thermal stimulation of the films upon irradiation with resonant laser light. Fig. 1 displays representative optical extinction spectra of an aqueous suspension and a PVA film containing gold nanorods. The typical transversal and longitudinal plasmonic bands are seen in the green and near infrared windows, respectively. The optical density roughly scales with the particle concentration, which increases by a factor of 20 upon drying and vertical compression of a 6% aqueous PVA sample.²⁵ Meanwhile, the plasmonic features undergo a significant red-shift and broadening, which may result from the interplay of the higher refractive index of PVA vs. water and plasmonic coupling at particle concentrations as high as 400 mM Au or inter-particle distances in the order of 100 nm.^{19,25}

According to the intrinsic properties of LN crystals, this thermal activation triggers local pyroelectric effects, which translate into intense electric fields.^{26,28} In this way, GNRs

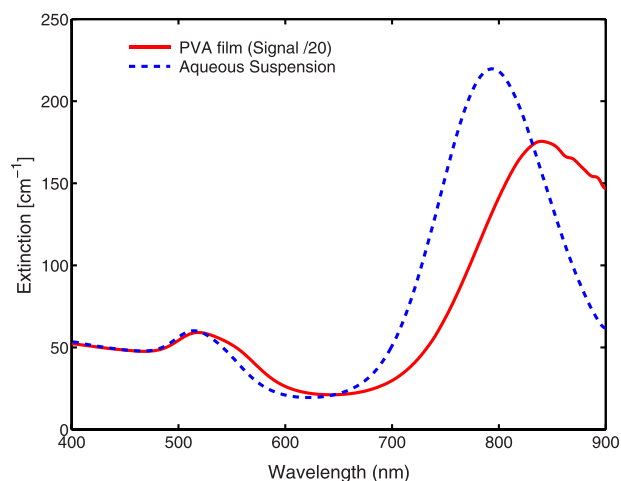


FIG. 1. Optical extinction spectra of an aqueous suspension (blue dotted line) and a PVA film (red continuous line) containing gold nanorods. For the sake of comparison, the optical density of the PVA film has been divided by a factor of 20 reflecting its higher particle concentration.

deposited onto the LN wafer (GNR-LN device) can be activated by NIR light to provide a cascade of photothermal and pyroelectric conversions. Fig. 2 shows the top view of the GNR-LN device used in this work, where an array of 3×3 films with 2 mm diameters was patterned.

The versatility and the reliability of the LA-EHD technique were investigated under three main configurations, as shown schematically in Fig. 3. Basically, three parallel and horizontal plates made the set-up: the base glass slide with the liquid reservoir; the target glass slide facing the base (at a distance of about 2 mm) and receiving the drawn droplets; the driving GNR-LN plate back-illuminated by the NIR source. Specifically, the light source consisted of a AlGaAs diode laser (Mod. WELD 800 El.En. S.p.A., Italy) emitting at 810 nm and launched into a 300 μ m core diameter optical fibre. The GNR films absorbed the impinging light almost totally, leaving less than 10% reflected. The electric field induced by the thermal treatment was able to exert a significant hydrodynamic pressure onto the underlying reservoir, thus leading to the dispensing of small droplets from the base plate to the target plate or even the formation of a bridge between the two plates.²⁹ A IR thermocamera (ThermoVision™ A20 M by FLIR Systems, Inc) revealed that temperature of the GNR in PVA film can reach up to 100 °C; at this temperature of the PVA patterned film, the target slide, on which the LN crystal is placed, is about 50 °C

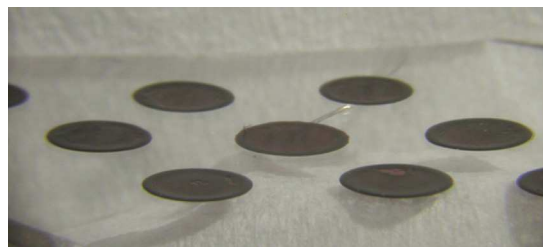


FIG. 2. Top view of an exemplary GNR-LN wafer used in this work. Nine PVA films containing a dispersion of GNRs are deposited onto a LN crystal wafer. The diameter size of the films is about 2 mm while the thickness ranges between 20 and 50 μ m. Inhomogeneities due to the so-called coffee stain effect are visible.

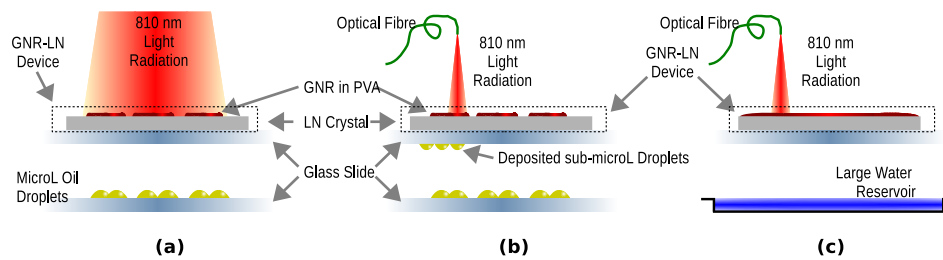


FIG. 3. Side view (not to scale) of the setup for the three experimental configurations used in this work. For all three schemes two microscope slides are mounted in parallel and horizontal. The GNR-patterned LN wafer is positioned on the upper slide with the GNR films on top. The lower slide hosts a set of drop or a macroscopic liquid reservoir. The distance between the GNR-LN device and liquid reservoir is about 2 mm. Laser radiation from an AlGaAs diode laser (Mod. WELD 800 El.En. S.p.A., Italy) at 810 nm is launched into a 300 μm core diameter optical fibre which is used to excite the GNR-LN device. (a) An entire pattern of films is illuminated at the same time, diameter of each film is about 2 mm. (b) Individual films are illuminated one at the time. (c) A large film (size 10 mm) is heated pointwise by light from a fibre tip and can activate dispensing from a large free surface reservoir.

colder. However, thanks to the versatility of the technique that allows one to use lower power laser and/or shorter illumination, such temperatures may be reduced further. Since the droplets dispensing is driven by the generated electric field, the LA-EHD technique works well when target plate and LN wafer are closed but not in contact; for instance, when they are at a distance of 100 μm , the target plate remains at room temperature and the experimental sequence is perfectly reliable.

The configurations displayed in Figs. 2(a) and 2(b) had both a separate distribution of the reservoir and of the GNRs on the LN crystal, with drops on the base and an array of (3×3) GNR on the driving plate. However, a single expanded beam excited simultaneously the GNR films in case (a), while a scanning small sized beam was used in (b) for single spot excitation. Therefore, in case (a) a multiple dispensing effect was obtained where sub-microliter droplets were drawn from the base selectively and, simultaneously, in correspondence of the patterned GNR spots. In case (b) the droplets were drawn separately from the base drops, thus obtaining a serial dispensing effect. Conversely, the configuration in (c) consisted of an extensive distribution of both the reservoir and the GNRs, with a free surface water reservoir as base (around 1 ml volume) and a homogeneous layer of GNRs (area around 1 cm^2) on the driving plate, excited locally by a scanning laser beam. In this way a serial dispensing effect was demonstrated also in case of large reservoir.

Fig. 4 shows the side view of typical multiple dispensing events. Five almond oil sessile droplets (about 1 μl each) are positioned on the lower glass slide in correspondence to the GNR spots on the driving plate, according to the configuration of Fig. 2(a). Laser radiation lighted an area of about 1.5 cm diameter with a 5.6 W power, so that the spots were illuminated simultaneously from above. Movie 4 shows the simultaneous activation of the drops during a 8 s long illumination event. Phenomena were captured by a CCD-camera (Dino-Eye AM423X). The response time was 2 s long (i.e., the time between the illumination start and the first droplet has been dispensed). It is possible to observe a sequence of liquid shootings where the base drops dispensed small daughter droplets onto the target slide. The average number of dispensed droplets is at a rate of about 1 every 2 s from a single reservoir drop.

The mechanism of drop deformation and break-up under an electric field is complex. Only recently Basaran and

coworkers²⁹ have presented a comprehensive physical model of EHD tip streaming, while the phenomenon is well known according to the Taylor-cone model.³⁰ The dynamic evolution shows that the reservoir drops first undergo deformation into a conical tip, with its height increasing under the pyro-EHD force, and then dispenses a droplet and relaxes in a cycle that is produced periodically until the electric field vanishes. The whole process consists in the simultaneous streaming of adjacent reservoir drops by the same optical stimulus in a multi dispensing system. According to the fundamentals of EHD,³¹ a critical value D_c exists for the distance D between the base and the driving plate

$$D_c = \left(1 + \frac{\theta}{4}\right) \sqrt[3]{V}, \quad (1)$$

where θ is the contact angle of the base drop onto the base plate and V is the volume of the drop reservoir. A stable liquid bridge establishes when $D < D_c$. In our setup $D > D_c$, a stable liquid bridge cannot be established but a liquid streaming regime occurs and the distance D and the volume of the drop reservoir can be slightly varied in order to control the volume of the dispensed droplets.¹⁴ For example, Movie 4 shows that a droplet of the order of 0.5 μl was dispensed at the beginning of the process, while smaller droplets (around

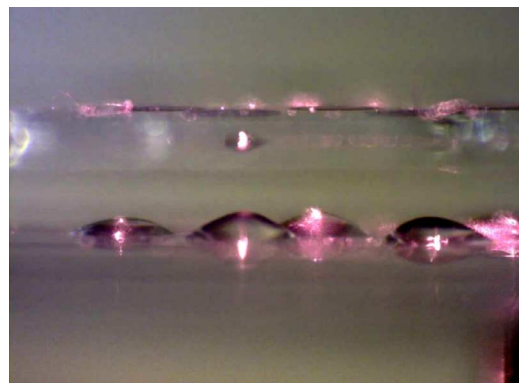


FIG. 4. Side view of a multi dispenser of five almond oil droplets (about 1 μl each). These drops are positioned on the lower glass slide right below the GNR films placed onto LN wafer. The distance between the two glass slides is 2 mm. Laser radiation lights an area of 1.5 cm diameter, so that the films are simultaneously illuminated from above. In the movie it is possible to see a sequence of liquid shootings where the almond oil drops dispense small droplets onto the above glass slide (enhanced online) [URL: <http://dx.doi.org/10.1063/1.4825337.1>].

0.1 μl) were dispensed at the end of the process, when the volume of the reservoir drop was reduced.

The second configuration (Fig. 2(b)) allowed us to bring the fibre tip very close to the GNR spots for illuminating them separately through mechanical scanning. Fig. 5 shows the base drops stimulated selectively and sequentially by the laser beam incident onto individual GNR spots. The dispensed droplets appeared to slip to colder region due to thermocapillarity,³² thus yielding a serial dispenser, which may be addressed by the optical fibre (see Movie 5). In the end of the sequence, a droplet from the rear row is seen to behave differently because of a change in the position of the reservoir drop with respect to the crystal. This reservoir drop dispensed a continuous thread of liquid, thus establishing a liquid bridge.³¹ In this configuration, the light power was set to 0.7 W. Each GNR spot was stimulated by a 4 s long irradiation, and the response time of the base drop (i.e., time range between irradiation start and first droplet) was 2 s. Each base drop appeared to dispense around 8 droplets for each irradiation event and the dispensing rate was evaluated to be around 4 droplets per second. These values point out that this configuration provides a faster process, thus improving the dispensing efficiency, mainly due to a better control on the light addressing with sufficient spatial resolution.

We have evaluated that 0.2 W is the minimum laser radiation incident power needed to trigger a stream of droplets from the reservoir. The PVA + GNR layer reflects less than 10% of this incident light energy and it extinguishes more than 95% of this energy light which is converted into heat by more than 90%.²⁷ The electric field appearing after a temperature change of the pyroelectric LN crystal relaxes mainly due to the screening of the polarization surface charges by charged particles adsorbed from the surrounding medium.²⁸ As the thermal mass of the absorber determine its response time in temperature, the minimum laser power can be lowered and the efficiency of the mechanism can be improved by using a thinner crystal (of the order of 10 μm) that could be difficult to handle and could change dramatically the geometry of the experiment.

With this experimental configuration it is also possible to evaluate the minimum droplet size achieved in this work.



FIG. 5. Serial dispenser from nine almond oil droplets (about 1 μl each). Reservoir drops from the bottom are stimulated selectively and sequentially one at the time by the laser beam incident on the single GNR disk-film on the front of the matrix. The distance between the two glass slides is 2 mm and the size of the optical fibre is 300 μm . In the movie it is possible to see that droplets in the middle and rear rows behaves in the same way thus yielding a serial dispenser which may be addressed with a fibre tip (enhanced online) [URL: <http://dx.doi.org/10.1063/1.4825337.2>].

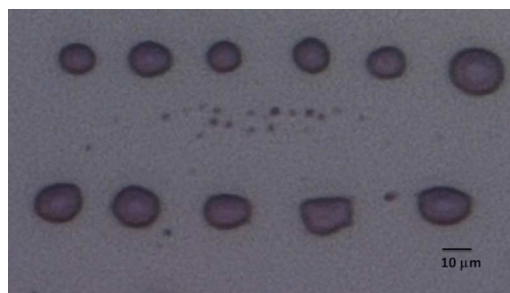


FIG. 6. Image of droplets collected on a glass plate at the end of sequence of streaming from a single reservoir drop. Dimensions of the smallest droplet are of the order of 10 μm .

Sequences of droplets shot from a single sessile reservoir drop are collected on a glass plate while the glass plate is horizontally moved. During the deposition, the volume of the reservoir drop was reducing and the volume of the deposited droplets as well. The smallest droplets are shown in Fig. 6 and they have dimensions of the order of 10 μm .

Another intriguing functionality of the device is the possibility of dispensing droplets from a free surface reservoir (instead of sessile drop) with high spatial resolution, as shown in the third configuration (Fig. 2(c)). Fig. 7 displays the side view of the dispensing event in case of a relatively large volume of water (around 1 ml) confined into a petri dish. In this case a uniform layer of GNRs was deposited onto the LN crystal with a diameter of about 10 mm. The optical fibre stimulated the GNR-LN wafer locally and the dynamic evolution shows that the surface of the liquid reservoir changed into a conical tip in correspondence of the stimulation spot. Such cone elongated further under the action of the pyro-EHD force, until the occurrence of the dispensing event (see Movie 7). In this case, the response time was 4 s long. Thanks to the high fidelity through which the jetting cone develops in correspondence of the stimulation spot, the technique provides the



FIG. 7. Droplet dispensing from a large reservoir. The GNR-LN comprises a single 10 mm large GNR film placed onto a LN crystal. The GNR-LN device is stimulated locally by laser light escaping from the tip of an optical fibre. Due to the pyro-electrohydrodynamic force the surface of the liquid reservoir has changed to exhibit a conical tip. The distance between the water surface (when it is not undergoing the electric field) and the upper glass slides is 2 mm and the size of the optical fibre is 300 μm . In the movie the fibre position is moved through different sites (enhanced online) [URL: <http://dx.doi.org/10.1063/1.4825337.3>].

possibility of drawing small amounts of liquid with high resolution from relatively large reservoirs.

In summary, we presented here a LA-EHD technique for drawing sub-microliter volumes of liquids using a pyro-EHD effect induced by plasmon resonance of GNRs. The resonance was achieved by NIR irradiation, thus enabling the direct activation of the pyroelectric effect into a LN crystal through a compact, versatile, and light source. In fact, thanks to the availability on one side of a laser exiting an optical fibre and, on the other side, of activation sites of the pyroelectric effect patterned directly onto the driving crystal, the dispensing is highly versatile and resolved. Both serial and multiple dispensing were demonstrated by playing with the degree of expansion of the beam, namely, by modulating simply the distance between the fibre and the GNR device. In addition, the fibre-based activation enables the stimulation of jetting cones with high fidelity and resolution, even in case of free surface reservoirs. Finally, the method is applicable to different kinds of liquids, including oil and water with a rather fast response. The possibility of using NIR laser for stimulating the EHD force opens the way for compact, cost-effective, and integrated systems with minimal interference with the solvents and reagents constituting the liquid droplets.

This work has been partially supported by the Project of the Health Board of the Tuscany Region “NANO-CHROM”. The authors acknowledge the Italian Ministry of Research for financial support, under the “Futuro in Ricerca 2010” Programme (Protocol RBFR10FKZH) and the EFOR-CABIR CNR project. The authors wish to thank Andrea Finizio for helpful discussions.

¹G. M. Whitesides, *Nature* **442**, 368 (2006).

²J. M. Köhler and T. Henkel, *Appl. Microbiol. Biotechnol.* **69**, 113 (2005).

³A. Huebner, S. Sharma, M. Srisa-Art, F. Hollfelder, J. B. Edel, and A. J. deMello, *Lab Chip* **8**, 1244 (2008).

⁴D. A. Sessoms, M. Belloul, W. Engl, M. Roche, L. Courbin, and P. Panizza, *Phys. Rev. E* **80**, 016317 (2009).

⁵M. A. Burns, C. H. Mastrangelo, T. S. Sammarco, F. P. Man, J. R. Webster, B. N. Johnsons, B. Foerster, D. Jones, Y. Fields, A. R. Kaiser, and D. T. Burke, *Proc. Natl. Acad. Sci. U.S.A.* **93**, 5556 (1996).

⁶B. S. Gallardo, V. K. Gupta, F. D. Egerton, L. I. Jong, V. S. Craig, R. R. Shah, and N. L. Abbott, *Science* **283**, 57 (1999).

⁷K. Ichimura, S.-K. Oh, and M. Nakagawa, *Science* **288**, 1624 (2000).

⁸T. B. Jones, M. Gunji, M. Washizu, and M. J. Feldman, *J. Appl. Phys.* **89**, 1441 (2001).

⁹S. Grilli, L. Miccio, V. Vespini, A. Finizio, S. De Nicola, and P. Ferraro, *Opt. Express* **16**, 8084 (2008).

¹⁰P. Ferraro, S. Grilli, L. Miccio, and V. Vespini, *Appl. Phys. Lett.* **92**, 213107 (2008).

¹¹A. Casner and J.-P. Delville, *Phys. Rev. Lett.* **90**, 144503 (2003).

¹²T. Ondarçuhu, J. Arcamone, A. Fang, H. Durou, E. Dujardin, G. Rius, and F. Pérez-Murano, *Eur. Phys. J. Spec. Top.* **166**, 15 (2009).

¹³J.-U. Park, M. Hardy, S. J. Kang, K. Barton, K. Adair, D. K. Mukhopadhyay, C. Y. Lee, M. S. Strano, A. G. Alleyne, J. G. Georgiadis *et al.*, *Nature Mater.* **6**, 782 (2007).

¹⁴P. Ferraro, S. Coppola, S. Grilli, M. Paturzo, and V. Vespini, *Nat. Nanotechnol.* **5**, 429 (2010).

¹⁵S. Grilli, S. Coppola, V. Vespini, F. Merola, A. Finizio, and P. Ferraro, *Proc. Natl. Acad. Sci. U.S.A.* **108**, 15106 (2011).

¹⁶V. Vespini, S. Coppola, S. Grilli, M. Paturzo, and P. Ferraro, *Lab Chip* **11**, 3148 (2011).

¹⁷P. Matteini, M. R. Martina, G. Giambastiani, F. Tatini, R. Cascella, F. Ratto, C. Cecchi, G. Caminati, L. Dei, and R. Pini, *J. Mater. Chem. B* **1**, 1096 (2013).

¹⁸F. Ratto, P. Matteini, A. Cini, S. Centi, F. Rossi, F. Fusi, and R. Pini, *J. Nanopart. Res.* **13**, 4337 (2011).

¹⁹P. Matteini, F. Ratto, F. Rossi, S. Centi, L. Dei, and R. Pini, *Adv. Mater.* **22**, 4313 (2010).

²⁰P. Matteini, F. Ratto, F. Rossi, M. de Angelis, L. Cavigli, and R. Pini, *J. Biophotonics* **5**, 868 (2012).

²¹F. Ratto, P. Matteini, F. Rossi, and R. Pini, *J. Nanopart. Res.* **12**, 2029 (2010).

²²B. Nikoobakht and M. A. El-Sayed, *Chem. Mater.* **15**, 1957 (2003).

²³F. Ratto, P. Matteini, S. Centi, F. Rossi, F. Fusi, and R. Pini, *Proc. SPIE* **7910**, 5954853 (2011).

²⁴R. D. Deegan, O. Bakajin, T. F. Dupont, G. Huber, S. R. Nagel, and T. A. Witten, *Nature* **389**, 827 (1997).

²⁵R. Mercatelli, F. Ratto, S. Centi, S. Soria, G. Romano, P. Matteini, F. Quercioli, R. Pini, and F. Fusi, *Nanoscale* **5**, 9645–9650 (2013).

²⁶M. Paturzo, P. Ferraro, S. Grilli, D. Alfieri, P. De Natale, M. De Angelis, A. Finizio, S. De Nicola, G. Pierattini, F. Caccavale, D. Callejo, and A. Morbiato, *Opt. Express* **13**, 5416 (2005).

²⁷R. Mercatelli, G. Romano, F. Ratto, P. Matteini, S. Centi, F. Cialdai, M. Monici, R. Pini, and F. Fusi, *Appl. Phys. Lett.* **99**, 131113 (2011).

²⁸A. V. Butenko, V. Sandomirsky, G. Chaniel, B. Shapiro, Y. Schlesinger, A. Jarov, and V. A. Sablikov, *J. Appl. Phys.* **108**, 044106 (2010).

²⁹P. K. Notz and O. A. Basaran, *J. Colloid Interface Sci.* **213**, 218 (1999).

³⁰G. Taylor, *Proc. R. Soc. London, Ser. A* **280**, 383 (1964).

³¹N. Maeda, J. N. Israelachvili, and M. M. Kohonen, *Proc. Natl. Acad. Sci. U.S.A.* **100**, 803 (2003).

³²B. Selva, V. Miralles, I. Cantat, and M.-C. Jullien, *Lab Chip* **10**, 1835 (2010).